Solving PDE's with FEniCS

Conservation Laws and Hyperbolic Systems

Chapters 23 and 24

Introduction to

Automated Modeling

with FEniCS

by L. Ridgway Scott

Conservation laws are PDEs of the form

$$\mathbf{u}_t(\mathbf{x}, t) + \nabla \cdot \mathbf{F}(\mathbf{u}(\mathbf{x}, t)) = 0. \tag{1}$$

- $\mathbf{x} \in \mathbb{R}^d$ for $d = 1, 2, 3$,
- $\mathbf{u} \in \mathbb{R}^n$ where n can be any positive integer, and
- $\mathbf{F}$ is a function defined on $\mathbb{R}^n$ with values in $\mathbb{R}^d$.

Thus $\nabla \cdot \mathbf{F}$ means

$$(\nabla \cdot \mathbf{F}(\mathbf{v}))_j = \sum_{k=1}^{d} F_{j,k}, \ \ j = 1, \ldots, n.$$

The simplest example is for $d = n = 1$, the **inviscid Burgers equation**

$$0 = u_t + \tfrac{1}{2}(u^2)_x = u_t + uu_x. \tag{2}$$

Here $F(v) = \frac{1}{2}v^2$.

In general, for $d = 1$ and $n = 1$, (1) becomes

$$u_t(x,t) + f(u(x,t))_x = 0. \tag{3}$$

We can think of the pair $U = (u, f(u))$ as a vector function of x and t.

In this notation, $u_t + f(u)_x = \nabla \cdot U$.

Define $\mathbb{R}_\pm = \{t \in \mathbb{R} \ : \ \pm t \geq 0\}$. Multiplying by a test function v and integrating over $\mathbb{R} \times \mathbb{R}^p$ we get

$$0 = \int_{\mathbb{R}} \int_{\mathbb{R}^p} (\nabla \cdot U) v \, dt \, dx. \tag{4}$$

Apply divergence theorem (2.9) to Uv on $\mathbb{R} \times \mathbb{R}^p$:

$$\begin{aligned}
-\int_{\mathbb{R}} u_0 v \, dx &= \int_{\mathbb{R}} \int_{\mathbb{R}^p} \nabla \cdot (Uv) \, dt \, dx \\
&= \int_{\mathbb{R}} \int_{\mathbb{R}^p} (\nabla \cdot U) v \, dt \, dx + \int_{\mathbb{R}} \int_{\mathbb{R}^p} U \cdot (v_t, v_x) \, dt \, dx \\
&= \int_{\mathbb{R}} \int_{\mathbb{R}^p} (u_t + f(u)_x) v \, dt \, dx + \int_{\mathbb{R}} \int_{\mathbb{R}^p} (u, f(u)) \cdot (v_t, v_x) \, dt \, dx.
\end{aligned} \tag{5}$$

Therefore

$$\begin{aligned} 0 &= \int_{\mathbb{R}} \int_{\mathbb{R}^p} (u_t + f(u)_x) v \, dt \, dx \\ &= -\int_{\mathbb{R}} \int_{\mathbb{R}^p} u v_t + f(u) v_x \, dt \, dx - \int_{\mathbb{R}} u_0 v \, dx. \end{aligned} \tag{6}$$

This yields the weak formula for the conservation law:

$$\int_{\mathbb{R}} \int_{\mathbb{R}^p} u v_t + f(u) v_x \, dt \, dx + \int_{\mathbb{R}} u_0 v \, dx = 0 \tag{7}$$

for smooth v vanishing outside a bounded set in $\mathbb{R} \times \mathbb{R}^p$.

Functions u satisfying (7) are called **weak solutions**.

Weak solutions

With elliptic equations, there is a strong correspondence between the weak solutions defined by the variational formulation and the strong form of the PDE.

However, for conservation laws, the situation is more complicated.

Indeed, the weak form of a conservation law does not fully specify their solution.

It has been observed that the “class of weak solutions associated with a given system of equations depends on the form in which the equations are written” [32, page 161].

Weak solution nonuniqueness

An example of the nonuniqueness for conservation laws is given in [32]: both

$$u(x,t) = \begin{cases} 0 & x < 0 \\ x/t & 0 < x < t \\ 1 & t < x \end{cases} \tag{8}$$

and

$$w(x,t) = \begin{cases} 0 & 2x < t \\ 1 & t < 2x \end{cases} \tag{9}$$

solve (7) for the inviscid Burgers equation.

We can verify that u is a solution:

$$u_t(x,t) = \begin{cases} 0 & x < 0 \\ -x/t^2 & 0 < x < t \\ 0 & t < x \end{cases}$$

and

$$u_x(x,t) = \begin{cases} 0 & x < 0 \\ 1/t & 0 < x < t \\ 0 & t < x \end{cases}.$$

Thus $uu_x = -u_t$ in each of the intervals $x < 0$, $0 < x < t$, and $x > t$.

Weak solutions

Thus $(u_t + uu_x, v)_{L^2(\Omega)} = 0$ for all smooth v.

Since u is continuous, and piecewise linear, we can integrate by parts to obtain (7).

The verification that w is a weak solution is complicated by the fact that it is discontinuous.

But the weak formula does not require continuity, and both ww_x and w_t are zero on the intervals $2x < t$ and $2x > t$.

We can revisit the divergence theorem in (5).

Weak solutions

Let us be slightly more general and assume that we have a candidate solution w that is piecewise smooth, with a jump only across a curve $(\xi(t), t)$ in $\mathbb{R} \times \mathbb{R}^p$.

For simplicity, assume that $\xi(0) = 0$. Define

$$\Omega_- = \{(x,t) \in \mathbb{R} \times \mathbb{R}^p \ : \ x < \xi(t)\} \quad \text{and} \quad \Omega_+ = \{(x,t) \in \mathbb{R}$$

Let $\Gamma = \{(x,t) \in \mathbb{R} \times \mathbb{R}^p \ : \ x = \xi(t)\}$.

As before, define $U = (w, f(w))$ and apply the divergence theorem to Uv separately on Ω_- and Ω_+ and add the result together:

$$
\begin{aligned}
-\int_{\mathbb{R}} u_0 v\,dx + \int_{\Gamma} [\mathbf{n}\cdot U] v\,ds &= \int_{\Omega_-} \nabla\cdot(Uv)\,dt\,dx \\
&\quad + \int_{\Omega_+} \nabla\cdot(Uv)\,dt\,dx \\
&= \int_{\mathbb{R}}\int_{\mathbb{R}^p} (\nabla\cdot U) v\,dt\,dx + \int_{\mathbb{R}}\int_{\mathbb{R}^p} U\cdot(v_t, v_x)\,dt\,dx \qquad (10) \\
&= \int_{\mathbb{R}}\int_{\mathbb{R}^p} (w_t + f(w)_x) v\,dt\,dx \\
&+ \int_{\mathbb{R}}\int_{\mathbb{R}^p} (w, f(w))\cdot(v_t, v_x)\,dt\,dx.
\end{aligned}
$$

Weak solutions

Here $[\phi]$ denotes jump of ϕ across Γ: boundary of $\Omega_\pm$ is $\Gamma \cup \mathbb{R}_\pm$, with the normals $\pm\mathbf{n}$ in the divergence theorem being equal and opposite for $\Omega_\pm$ on Γ.

To be a weak solution, we must have

$$[\mathbf{n} \cdot U] = 0 \quad \text{on } \Gamma.$$

This is known as the **Rankine–Hugoniot** condition.

The vector $(\xi'(t), 1)$ is tangent to Γ, so the normals to Γ are $\pm c(t)(-1, \xi'(t))$, where

$$c(t) = \sqrt{1 + \xi'(t)^2}.$$

Thus we can write the **jump condition** as

$$w_+ - w_- = \big(f(w_+) - f(w_-)\big)\xi'(t). \tag{11}$$

The proposed solution w satisfies $w_- = 0$ and $w_+ = 1$, and $\xi'(t) = 2$, so this reduces to

$$1 = f(1)\xi'(t) = \tfrac{1}{2} \cdot 2.$$

This completes the verification that w is a weak solution of the inviscid Burgers equation.

Weak solutions

Since the variational equation does not define the solution, some rule must be adopted to sort things out.

However, there is no universal way to determine relevant weak solutions.

Some have argued that there must be a solution determined by Nature.

The thinking is that the conservation law models a natural phenomenon and thus it should have a unique, natural solution.

But there could be many microscopic models of natural phenomenon leading to the same macroscopic model, so there is no “natural” criterion to choose one.

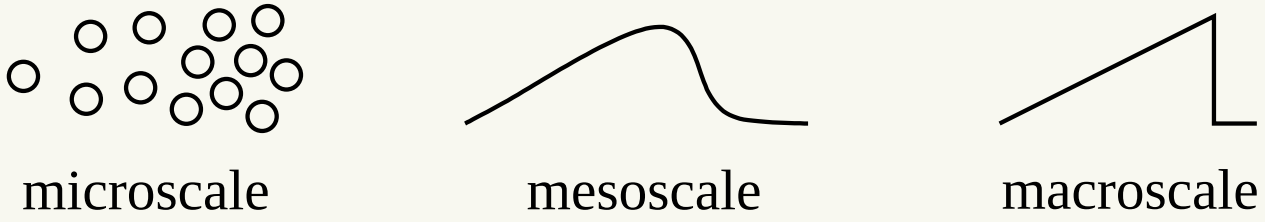

Figure 1: Different descriptions of matter. From the left: microscopic (e.g., molecules in a gas), mesoscopic (e.g., density of molecules described via continuum description), macroscopic (idealized limit of mesoscopic description).

Diffusion limits

Conservation laws represent the macroscale level in a multiscale model for many physical systems [21, 38], as depicted in Figure 1.

One such system models the dynamics of a gas [5, 34].

The microscale model in this case is a molecular model [21].

In many cases, the microscale model can be well approximated at a mesoscale as an advection–diffusion system.

For Burgers equation, resulting equation is

$$0 = u_t + uu_x - \epsilon u_{xx}. \tag{12}$$

This is called the **viscous Burgers equation**.

In many cases, it makes sense to take the limit as $\epsilon \to 0$, obtaining what are called **viscosity solutions** [20].

Hamilton–Jacobi equations generalize the concept of conservation laws and take the form

$$u_t(\mathbf{x}, t) + H(\mathbf{x}, \mathbf{u}(\mathbf{x}, t), \nabla \mathbf{u}(\mathbf{x}, t)) = 0.$$

Viscosity solutions first developed in this framework [20] and generalized to second-order PDEs [19].

Solving the viscous Burgers equation

Let us consider solving (12) with initial conditions appropriate for the proposed solutions (8).

We will shift the origin by one-half, and take the initial condition to be

$$u_0(x) = \tfrac{1}{2}(1 + \tanh(K(x - \tfrac{1}{2}))$$

for a suitably large value of K.

Viscous Burgers example

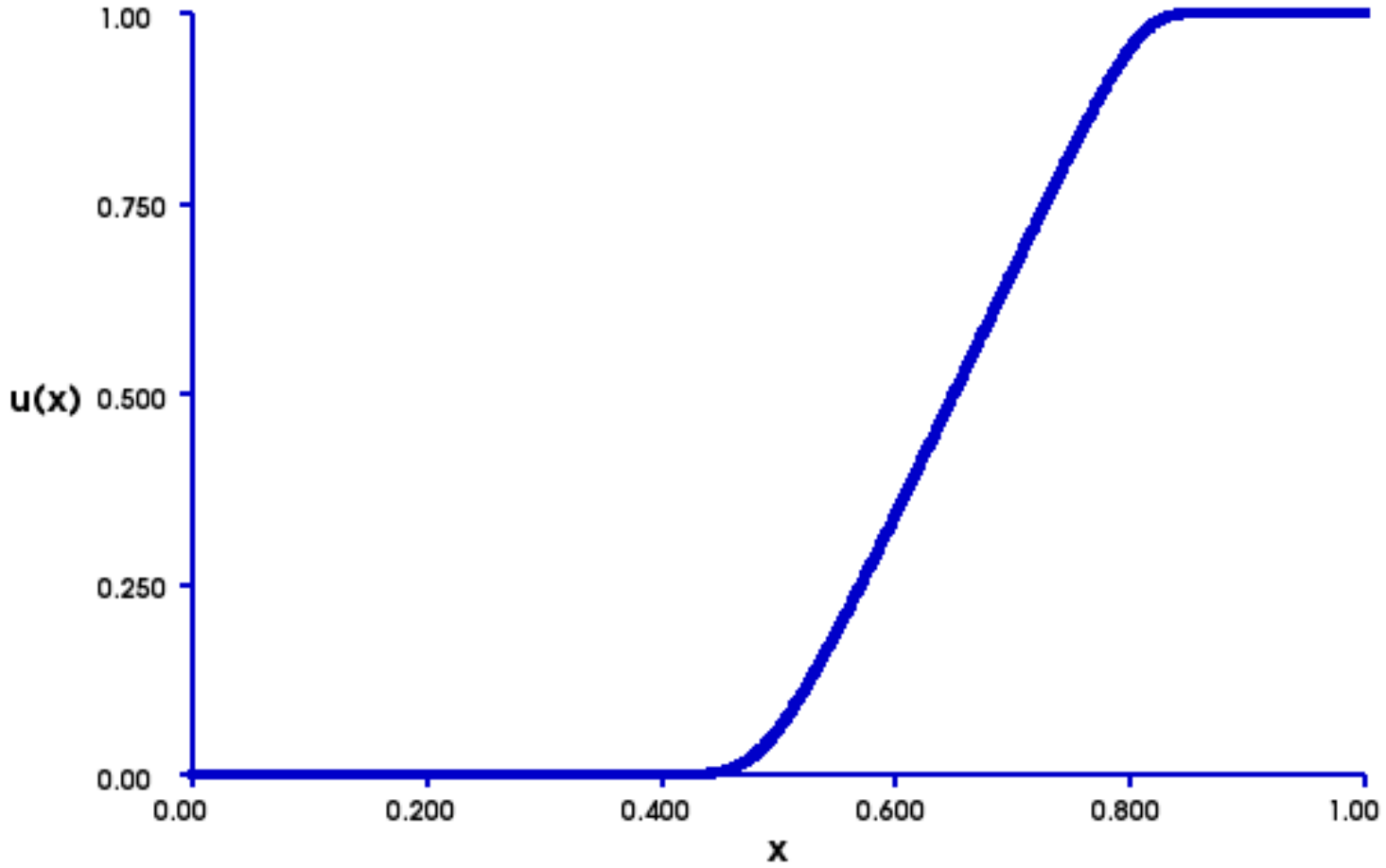

Figure 2: Solution of (12) on $[0, 1]$ by piecewise linears using the algorithm (13) with 1000 mesh points, $\Delta t = 0.001$, and $\epsilon = 10^{-3}$. Initial condition $u_0(x) = \frac{1}{2}(1 + \tanh(10^5(x - \frac{1}{2}))$. Solution is shown at $T = 0.3$.

To simplify the approximation, we modified the implicit Euler scheme (10.34) for the heat equation to obtain

$$\begin{aligned}(u^{n+1},v)_{L^2(\Omega)} + \Delta t\big(a_\epsilon(u^{n+1},v) + (u^{n+1}u_x^n,v)_{L^2(\Omega)}\big)\\ = (u^n,v)_{L^2(\Omega)} \quad \forall v\in V,\end{aligned} \tag{13}$$

where

$$a_\epsilon(w,v) = \epsilon\int_\Omega w'(x)v'(x)\,dx = \epsilon\int_\Omega w_x(x)v_x(x)\,dx.$$

Here we approximated the nonlinear term uu_x via

$$u^{n+1}u_x^n.$$

Viscous Burgers picks right solution

We see in Figure 2 that the viscosity method picks the solution u in (8) even though it has a more complex structure than w.

The code to produce Figure 2 and Figure 3 is in Program 23.2.

Viscous Burgers plots

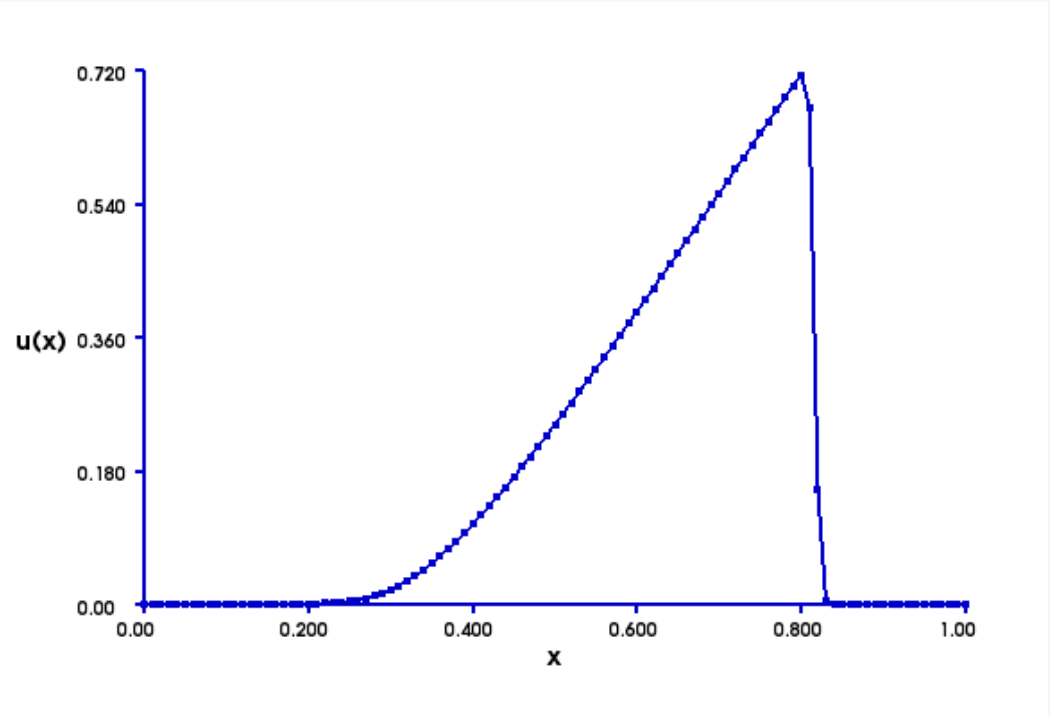

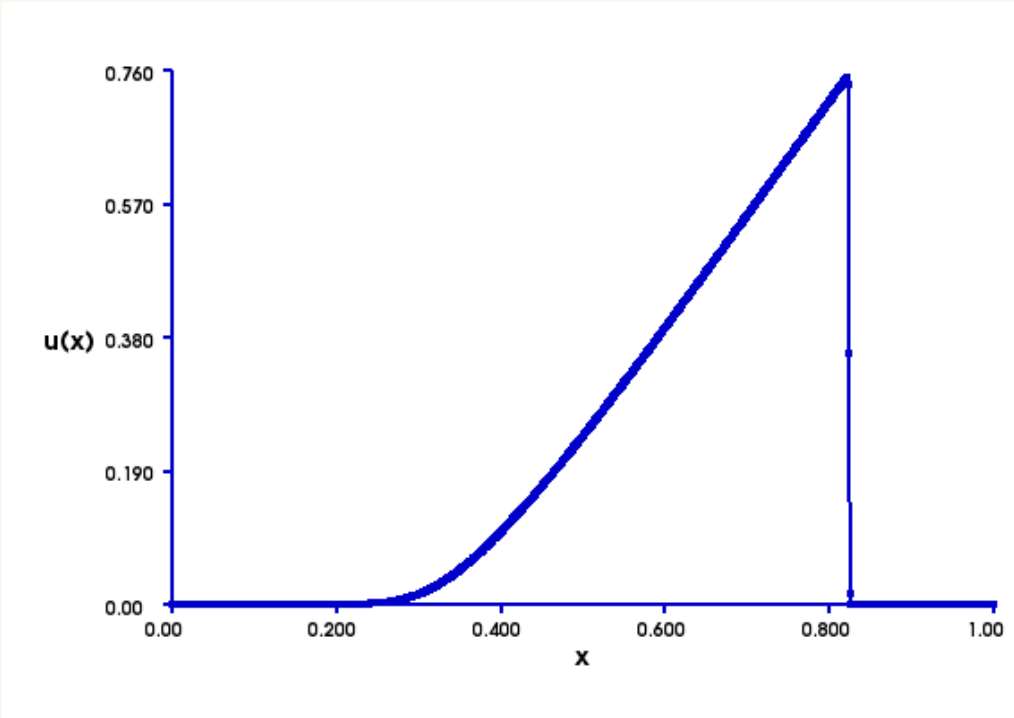

Figure 3: Solution of (12) on $[0, 1]$ by piecewise quartics using the algorithm (13). Initial condition $u_0(x) = e^{-(10x)^2}$. Solution is shown at $T = 0.5$. (Left) 100 mesh intervals, $\Delta t = 0.0001$, and $\epsilon = 10^{-3}$. (Right) 1000 mesh intervals, $\Delta t = 0.00005$, and $\epsilon = 10^{-4}$.

Smooth initial data

Using (13), we can investigate the behavior of Burgers' equation for different initial data.

In Figure 3, we show the solution with a Gaussian as initial data.

What happens is quite different from what we saw with other wave equations.

The solution is approaching a discontinuity on the front of the wave.

The back side approaches a linear ramp as seen in Figure 2.

Numerical nonuniqueness

In Section 9.5, we saw that nonlinear equations can have solutions whose data agree to within round-off error yet are globally quite different. Consider the related problem

$$\frac{du}{dt}(t,x) - \epsilon\frac{d^2u}{dx^2}(t,x) + u(t,x)\frac{du}{dx}(t,x) = 0 \quad \text{for } x \in [0,1],\ t \in$$
$$\frac{du}{dx}(t,0) = 0, \quad \frac{du}{dx}(t,1) = 0,$$
$$u(0,x) = \phi(x), \tag{14}$$

where $\epsilon > 0$ is a fixed parameter.

Weak solutions

The corresponding time-independent problem (9.18) was studied in Section 9.5 on the interval $[-1, 1]$.

In [8], it was shown that, if u is a solution of (14) such that $u(t, x) \to v(x)$ as $t \to \infty$ then v is a constant.

More precisely, they show that if $v \in L^2(0, 1)$ satisfies

$$\|u(t, \cdot) - v\|_{L^2(0,1)} \to 0 \text{ as } t \to \infty,$$

then v is constant.

Constants are time-independent solutions of (14).

Compare the results of [30, 37].

On the other hand, numerical evidence is presented in [8] that there are solutions of (14) that appear to tend to time-independent solutions, for example, for $\phi(x) = 5\cos(\pi x)$ and $\phi(x) = 50(\frac{1}{2} - x)^3$, with $\epsilon = 0.1$.

They show that the limiting numerical functions v are of the form

$$v_\beta(x) = -\beta \tanh((\beta/2\epsilon)(x - \tfrac{1}{2})), \qquad (15)$$

where the coefficient β is determined based on the computed solution.

v does not satisfy Neumann conditions in (14) exactly, but discrepancy is exponentially small, as in Section 9.5.

Review of wave equations

The simplest wave model (see Section 12.2) is

$$u_t + cu_x = 0, \tag{16}$$

where $c =$ wave speed. Solutions of this equation satisfy

$$u(t, x) = v(x - ct).$$

Solutions of nonlinear advection equations of the form

$$0 = u_t + f(u)_x = u_t + f'(u)u_x$$

no longer just translate to the right.

Review of wave equations, continued

Things move to the right at speeds $c(t,x) = f'(u(t,x))$ that depend on the size of u, and they can change shape, as seen in Figure 3.

Thus linear and nonlinear conservation laws are very different in character.

Finite difference approximation

We can approximate u on a grid in space and time:

$$u(i\Delta t, j\Delta x) \approx u_{i,j}.$$

We write

$$u_t(i\Delta t, j\Delta x) \approx \frac{u_{i,j} - u_{i-1,j}}{\Delta t}$$

$$f(u)_x(i\Delta t, j\Delta x) \approx \frac{f(u)_{i,j} - f(u)_{i,j-1}}{\Delta x}.$$

Thus we obtain the **upwind scheme**

$$u_{i+1,j} = u_{i,j} - \frac{\Delta t}{\Delta x}\left(f(u)_{i,j} - f(u)_{i,j-1}\right). \qquad (17)$$

This finite-difference approximation allows us to simulate nonlinear advection as easily as linear advection.

Notice that the scheme depends only on the ratio $\Delta t/\Delta x$, often referred to as the **CFL number** in honor of a paper by Courant, Friedrichs, and Lewy [18].

In Figure 4 we show the solution of the inviscid Burgers equation (2),

$$0 = u_t + \tfrac{1}{2}(u^2)_x,$$

with the same Gaussian initial data as in Figure 3.

Weak solutions

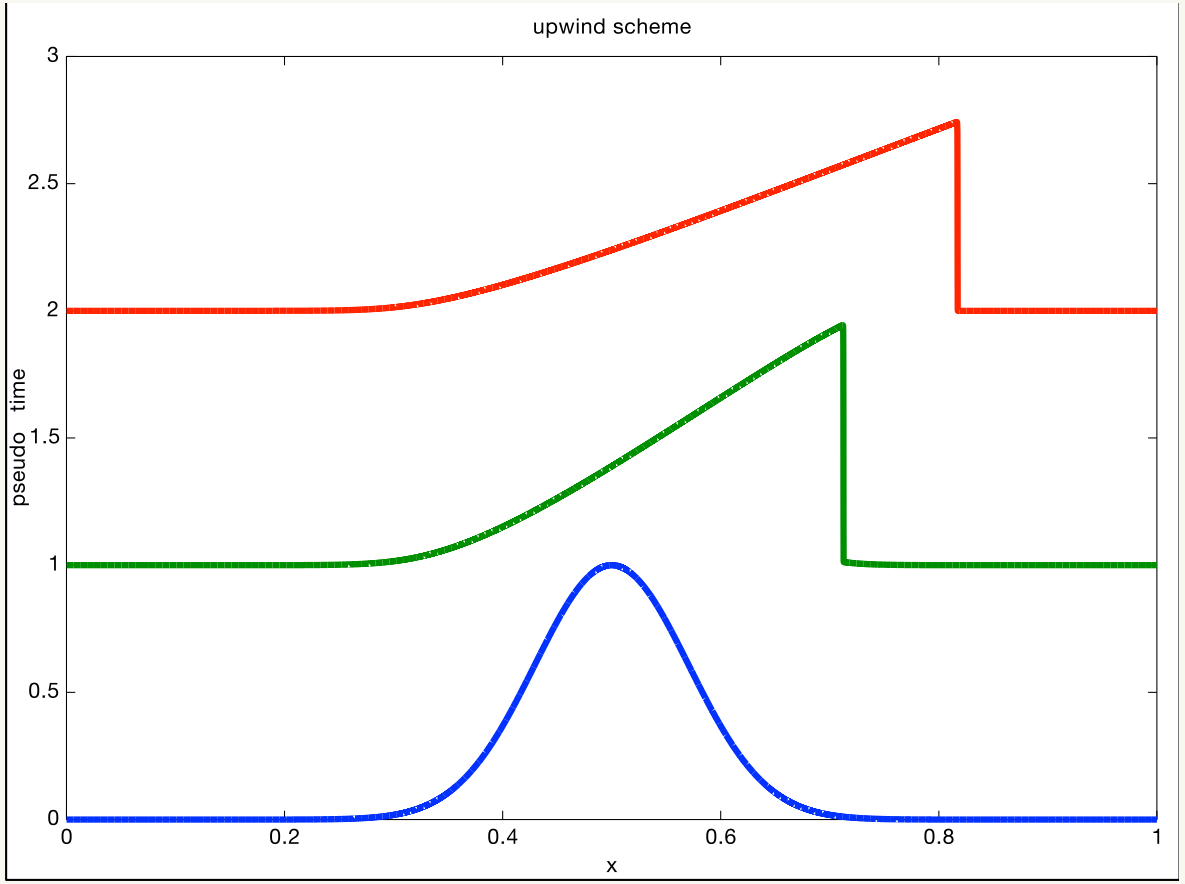

Figure 4: Solution of (2) on $[0, 1]$ by the upwind scheme (17) with 10^4 mesh points and $\Delta t/\Delta x = 0.1$. Initial condition $u_0(x) = e^{-(10x)^2}$. Solution is shown at $T = 0, .25, .5$. The vertical axis represents a pseudo time give by $4T$ chosen to avoid intersection of the curves. The `octave` code to produce this plot is given in Program 23.1.

Integral invariants

Let us consider solutions of conservation laws with finite support in space.

Although the wave shape changes with time, the integral of u is preserved: integrating the advection equation in space (and integrating by parts) gives

$$\frac{\partial}{\partial t}\int_{\mathbb{R}} u\,dx = \int_{\mathbb{R}} u_t\,dx = -\int_{\mathbb{R}} f(u)_x\,dx = 0. \tag{18}$$

Thus the area under the graph of u is constant. In Figure 4, we see that the initial wave forms convert to a long triangular form, and so its amplitude must decrease to maintain a constant area.

The integral of u^2 is also preserved: multiplying the advection equation by u and integrating in space (and integrating by parts) gives

$$\begin{aligned}\frac{1}{2}\frac{\partial}{\partial t}\int_{\mathbb{R}} u^2\,dx &= \int_{\mathbb{R}} uu_t\,dx = -\int_{\mathbb{R}} f(u)_x u\,dx \\ &= \int_{\mathbb{R}} f(u)u_x\,dx = \int_{\mathbb{R}} g(u)_x\,dx = 0,\end{aligned} \tag{19}$$

where $g' = f$, that is, g is an antiderivative of f, with $g(0) = 0$.

Shocks

Shocks can be described as discontinuities that can form and move, as shown in Figure 4, again with $f(u) = u^2$.

Shock fronts stay sharp, but back side of advancing wave remains continuous, as in Figure 4.

The amplitude has to decrease since the integrals of u and u^2 remain constant.

Over time, the wave amplitude goes to zero.

This is further illustrated on the left side of Figure 5 which has a step-function initial data.

Linear versus nonlinear shocks

In the linear case (16), even discontinuous solutions are propagated by translation:

$$u(t, x) = v(x - ct).$$

Even though the exact solution is trivial, let's see what our upwind difference method produces.

On the right side of Figure 5 we show the result of the upwind difference method (17) for $f(u) = u$.

In the case of linear advection, our numerical method produces waves that are no longer sharp at either the leading edge or trailing edge of a discontinuity.

Weak solutions

By contrast, the leading edge of the numerically computed nonlinear wave is sharp.

On the other hand, since the wave speed is constant, the linear waves move much faster than the nonlinear waves.

Thus difference methods treat linear and nonlinear waves quite differently.

Weak solutions

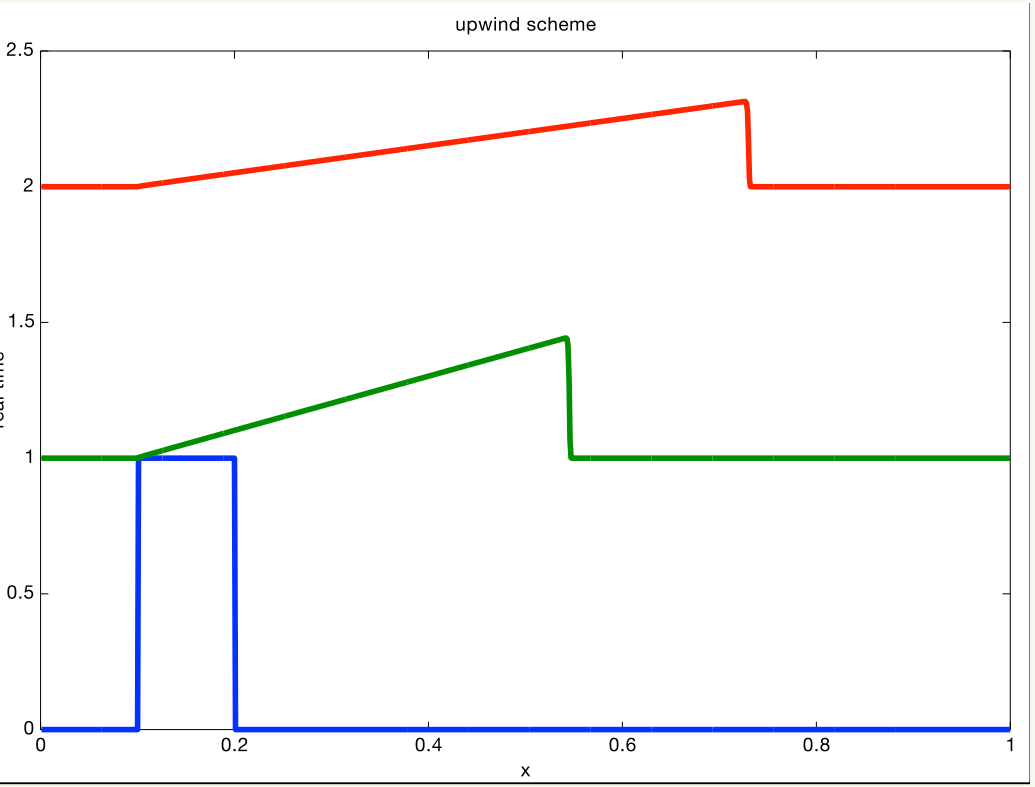

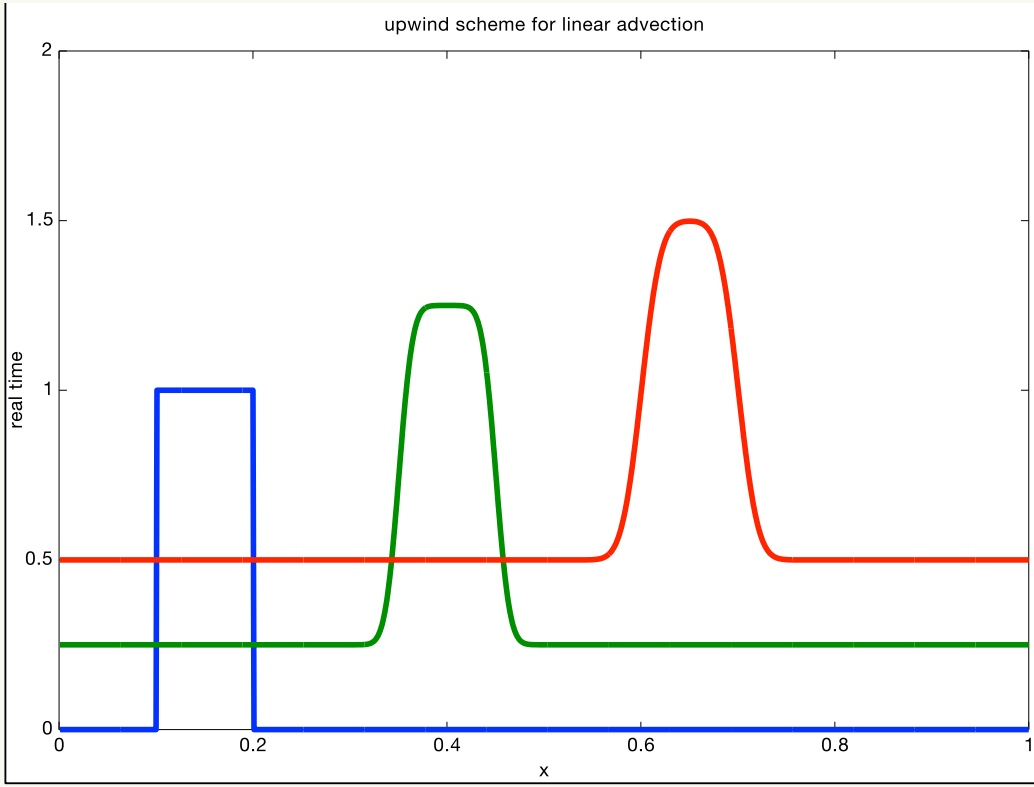

Figure 5: Upwind scheme with CFL=0.5, $\Delta x = 10^{-3}$ for (left) inviscid Burgers equation (2) and (right) linear advection (16) with speed $c = 1$.

Numerical dissipation

Numerical schemes for conservation laws introduce implicit dissipation. Taylor's approximation says

$$\frac{u_{i,j} - u_{i,j-1}}{\Delta x} \approx u_x(i\Delta t, j\Delta x) + \frac{\Delta x}{2} u_{xx}(i\Delta t, j\Delta x). \quad (20)$$

Thus the difference scheme is actually a better approximation to

$$u_t + u_x - \frac{\Delta x}{2} u_{xx} = 0$$

than it is to the linear advection equation

$$u_t + u_x = 0.$$

Weak solutions

In this case, we see [29, 11] that the difference method effectively introduces a diffusion or dissipation element, where the size of the diffusion constant depends on the mesh size.

Thus the difference method naturally picks out the diffusion-limit solution.

In the nonlinear case, we have

$$0 = u_t + f(u)_x - \frac{\Delta x}{2} f(u)_{xx}.$$

For the inviscid Burgers equation, this becomes

$$\begin{aligned} 0 &= u_t + uu_x - \frac{\Delta x}{2}\big(uu_x\big)_x \\ &= u_t + uu_x - \frac{\Delta x}{2}\big((u_x)^2 + uu_{xx}\big). \end{aligned} \tag{21}$$

The effect of the dissipation term is harder to predict in this case, but apparently it does not lead to excessive smoothing of shocks, contrary to the linear case.

We leave as an exercise

One key point is that the dissipation term in variational form turns off when $u = 0$.

Second-order dissipation

The second-order derivative term in

$$u_t + f(u)_x - \epsilon f(u)_{xx} = 0$$

is called a dissipation term: multiply the equation by u, integrate in space and integrate by parts to get

$$\begin{aligned} 0 &= \frac{1}{2}\frac{\partial}{\partial t}\int_{\mathbb{R}} u^2\,dx - \epsilon\int_{\mathbb{R}} u f(u)_{xx}\,dx \\ &= \frac{1}{2}\frac{\partial}{\partial t}\int_{\mathbb{R}} u^2\,dx + \epsilon\int_{\mathbb{R}} (u_x)^2 f'(u)\,dx, \end{aligned} \tag{22}$$

as in (19). Thus the integral of u^2 must dissipate to zero, since its time derivative is strictly negative (assuming that u is not identically constant and $f'(u) > 0$).

Artificial compression

The behavior depicted in Figure 5 suggests that nonlinearity controls diffusion artifacts.

Harten advocated artificial compression [40] as a means of reducing numerical dissipation.

Lax-Wendroff

Possible to alter numerical modifications in difference methods, but not eliminate them [11, 2].

For example, the Lax-Wendroff scheme for linear $f(u) = u$ [31, 33] is

$$u_{i+1,j} = \sum_{k=-1}^{1} b_k u_{i,j+k}, \tag{23}$$

where $b_{\pm 1} = \frac{1}{2}\alpha(\alpha \mp 1)$ and $b_0 = 1 - \alpha^2$, where $\alpha = \Delta t/\Delta x$ is the CFL number.

Numerical dispersion

The Lax-Wendroff scheme is second-order accurate in space, and it is a better approximation to

$$u_t + u_x - \gamma \Delta x^2 u_{xxx} = 0 \tag{24}$$

than it is to $u_t + u_x = 0$.

We leave as an exercise to compute γ.

Dispersion terms

The third-order derivative term in

$$u_t + f(u)_x - \epsilon u_{xxx} = 0 \tag{25}$$

is called a dispersion term (see Section 12.4).

Multiply the dispersion term by u, integrate in space and integrate by parts to get

$$\int u u_{xxx}\, dx = -\int u_x u_{xx}\, dx = -\int \tfrac{1}{2}((u_x)^2)_x\, dx = 0.$$

In view of (19), we conclude that the integral of u^2 is conserved for the solution u of (25).

Numerical errors

There has been a long quest to achieve more accuracy in numerical methods for conservation laws.

Although the upwind scheme (17) is quite effective, as we have seen, there has been significant interest in more accurate schemes.

The Lax-Wendroff [31, 33] scheme (23) is an early example.

Discontinuous Galerkin etc.

More recently, **discontinuous Galerkin** (DG) schemes have been widely studied [39].

DG schemes were first used in the context of models for advection terms in neutron transport (see references in [36]).

Even more recently, Galerkin schemes using continuous finite elements have been studied [27, 26, 25, 24, 23, 4].

Another new approach to conservation laws has been developed called **kinetic schemes** [3]. An example of their use is given in [14].

Hyperbolic Systems

Systems of hyperbolic conservation laws arise in many applications.

Perhaps simplest are the isentropic Euler equations.

These consist of two equations, one for the density of a gas and the other for the velocity (or momentum).

They are ostensibly defined in 3 space dimensions, but there are flows that are constant in some dimensions, so the system makes sense in 1 and 2 spatial dimensions as well.

We begin with the one-dimensional case.

Hyperbolic systems in one-D

Primary new phenomenon: waves can propagate in multiple directions and with different speeds.

No clear direction that is “upwind” in typical problems.

Moreover, shocks can collide.

In the two-dimensional case, a complication arises that does not at the moment have a simple resolution.

Multiple solutions arise after shocks collide.

No known way to (1) select one solution theoretically or (2) compute reliable solutions numerically.

The behavior of a gas moving in one direction at high speed can be modeled via

$$\begin{aligned} \rho_t + (\rho u)_x &= 0 \\ (\rho u)_t + (\rho u^2 + p(\rho))_x &= 0, \end{aligned} \tag{26}$$

where ρ is the density of the gas, u is the velocity in the x direction, and p is the pressure.

It is assumed that the pressure depends in an explicit way on the density.

A common choice for the pressure p is $p(\rho) = a\rho^\gamma$, where a and γ are constants satisfying $a > 0$ and $\gamma \geq 1$.

Modeling details

In this setting, it is assumed that the density and velocity are independent of the y and z directions.

Such behavior is approximated in a shock tube [41].

We assume that the domain of x is $\mathbb{R}$ and $t \geq 0$.

New variables

If we define $w = \rho u$, then the system (26) becomes

$$\begin{aligned} \rho_t + w_x &= 0 \\ w_t + (\rho^{-1} w^2 + p(\rho))_x &= 0, \end{aligned} \tag{27}$$

which is of the form (1), where

$$\mathbf{u} = \begin{pmatrix} \rho \\ w \end{pmatrix} \qquad \text{and} \qquad \mathbf{F} = \begin{pmatrix} w \\ \rho^{-1} w^2 + p(\rho) \end{pmatrix}.$$

This is often called the **conservation form** of the equations.

It has the defect that the vacuum state $\rho = 0$ [34] corresponds to a singularity.

Example solution

In order to understand better key aspects of hyperbolic systems, we consider an example.

If we take $\gamma = 3$, then (26) can be written [14] as two Burgers equations.

In particular, assume that

$$p(\rho) = \tfrac{1}{12}\rho^3.$$

Equivalent formulation

Define

$a(t,x) = u(t,x) + \frac{1}{2}\rho(t,x)$ and $b(t,x) = u(t,x) - \frac{1}{2}\rho(t,x)$.

First rewrite (26) as

$$\rho_t = -(\rho u)_x \qquad - u(\rho u)_x + \rho u_t + (\rho u^2 + \tfrac{1}{12}\rho^3)_x = 0.$$

The second equation can be simplified to

$$0 = u\rho u_x + \rho u_t + \tfrac{1}{4}\rho^2\rho_x = \rho\big(uu_x + u_t + \tfrac{1}{4}\rho\rho_x\big).$$

Example details

Then

$$\begin{aligned} a_t + aa_x &= u_t + \tfrac{1}{2}\rho_t + \big(u + \tfrac{1}{2}\rho\big)\big(u_x + \tfrac{1}{2}\rho_x\big) \\ &= u_t - \tfrac{1}{2}(\rho u)_x + uu_x + \tfrac{1}{2}\big(\rho u_x + u\rho_x\big) + \tfrac{1}{4}\rho\rho_x \\ &= u_t + uu_x + \tfrac{1}{4}\rho\rho_x = 0, \end{aligned} \tag{28}$$

assuming $\rho > 0$. Similarly

$$\begin{aligned} b_t + bb_x &= u_t - \tfrac{1}{2}\rho_t + \big(u - \tfrac{1}{2}\rho\big)\big(u_x - \tfrac{1}{2}\rho_x\big) \\ &= u_t + \tfrac{1}{2}(\rho u)_x + uu_x - \tfrac{1}{2}\big(\rho u_x + u\rho_x\big) + \tfrac{1}{4}\rho\rho_x \\ &= u_t + uu_x + \tfrac{1}{4}\rho\rho_x = 0. \end{aligned} \tag{29}$$

Note that

$$\rho = a - b, \quad u = \tfrac{1}{2}(a + b), \text{ and } w = \rho u = \tfrac{1}{2}\big(a^2 - b^2\big).$$

Plot equivalent solution

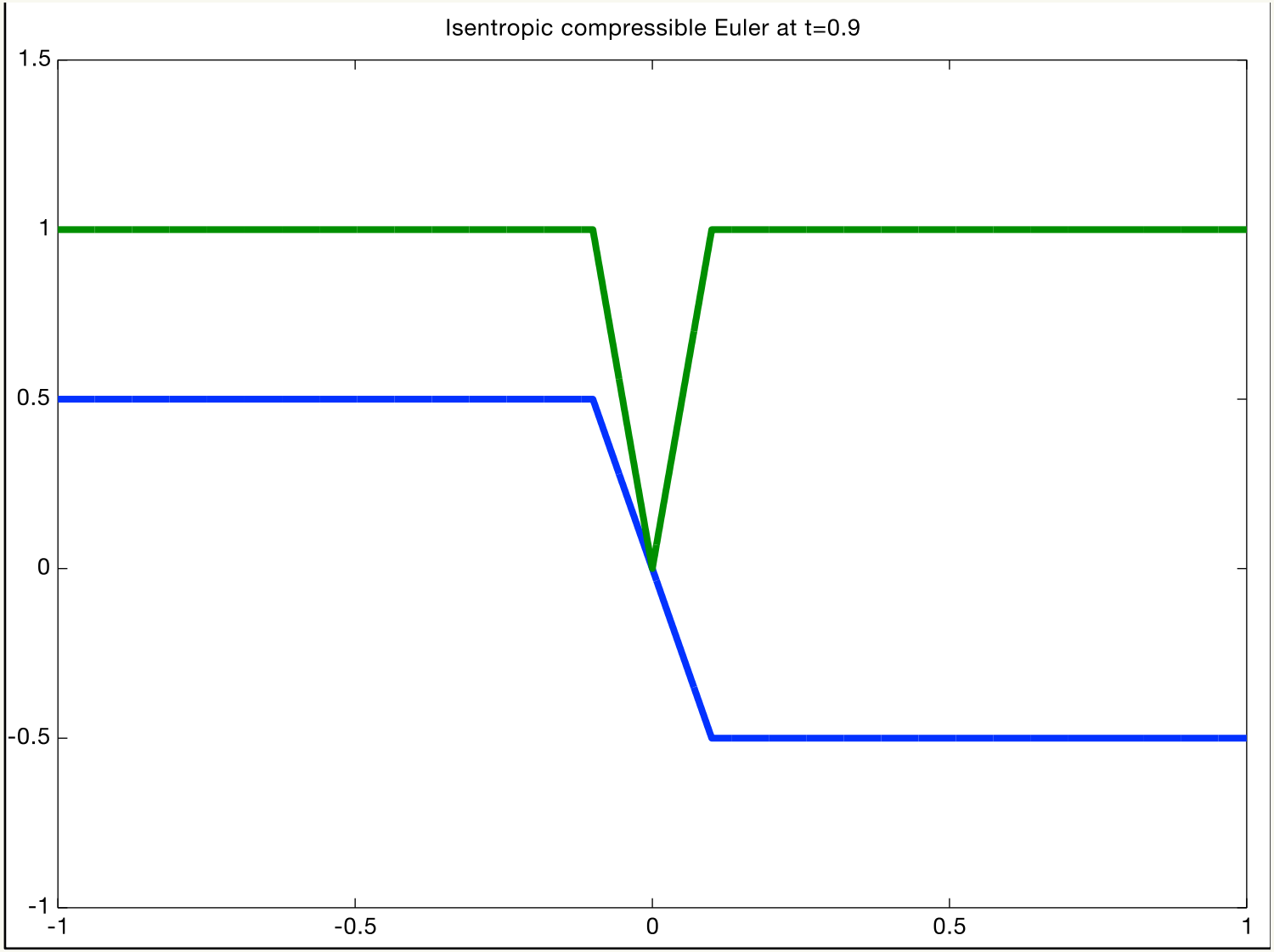

Figure 6: Solutions (34) at $t = 0.9$.

Initial data chosen

Following [14], define initial data

$$a_0(x) = \begin{cases} 1 & x \leq -1 \\ -x & -1 \leq x \leq 0 \\ 0 & x \geq 0 \end{cases},$$

and

$$b_0(x) = a_0(x-1) - 1 = \begin{cases} 0 & x \leq 0 \\ -x & 0 \leq x \leq 1 \\ -1 & x \geq 1 \end{cases}.$$

Initial data revealed

This corresponds to initial data for ρ and u of the form

$$\rho_0(x) = \begin{cases} 1 & |x| \geq 1 \\ |x| & |x| \leq 1 \end{cases}$$

and

$$u_0(x) = \begin{cases} \frac{1}{2} & x \leq -1 \\ -\frac{1}{2}x & -1 \leq x \leq 1 \\ -\frac{1}{2} & x \geq 1 \end{cases} .$$

Proposed solution for a

For $0 \leq t < 1$,

$$a(t,x) = \begin{cases} 1 & x \leq t-1 \\ -x/(1-t) & -1+t \leq x \leq 0 \\ 0 & x \geq 0, \end{cases} \tag{30}$$

and then for $t \geq 1$,

$$a(t,x) = \begin{cases} 1 & x \leq 2(t-1) \\ 0 & x > 2(t-1) \end{cases}. \tag{31}$$

We can verify that (30) satisfies $a_t = -aa_x$ as follows.

Differentiating with respect to t and x, we get

$$a_t(t,x) = \begin{cases} 0 & x \le t-1 \\ -x/(t-1)^2 & -1+t \le x \le 0 \\ 0 & x \ge 0, \end{cases},$$

$$a_x(t,x) = \begin{cases} 0 & x \le t-1 \\ 1/(t-1) & -1+t \le x \le 0 \\ 0 & x \ge 0, \end{cases}.$$

Multiplying the formula for a_x times (30) yields the formula for $-a_t$. We leave as Exercise 0.1 to show that (31) satisfies the Rankine-Hugoniot (weak solution) jump condition (11).

b is similar

Similarly, for $0 \leq t < 1$,

$$b(t,x) = \begin{cases} 0 & x \leq 0 \\ -x/(1-t) & 0 \leq x \leq 1-t \\ -1 & x \geq 1-t, \end{cases} . \tag{32}$$

and for $t \geq 1$,

$$b(t,x) = \begin{cases} 0 & x \leq 2(1-t) \\ -1 & x > 2(1-t) \end{cases} . \tag{33}$$

Back to u and ρ

Rewriting this in terms of u and ρ, we get for $0 \leq t < 1$

$$u(t,x) = \begin{cases} \frac{1}{2} & x \leq t-1 \\ -\frac{1}{2}x/(1-t) & t-1 \leq x \leq 1-t \\ -\frac{1}{2} & x \geq 1-t \end{cases},$$

$$\rho(t,x) = \begin{cases} 1 & x \leq t-1 \\ |x|/(1-t) & t-1 \leq x \leq 1-t \\ 1 & x \geq 1-t \end{cases}.$$

These solutions are depicted in Figure 6 at $t = 0.9$.

Getting past the shock

Unfortunately, the equivalence of (a, b) and (u, ρ) does not extend past $t = 1$ where the shocks collide, due to the discontinuity of u in x that appears at $t = 1$.

Starting at $t = 1$, we have what is called a **Riemann problem**, with initial data

$$\rho_\pm = 1 \text{ and } u_\pm = \pm\tfrac{1}{2}.$$

That is, we have

$$u(1,x) = \begin{cases} \frac{1}{2} & x < 0 \\ -\frac{1}{2} & x > 0 \end{cases}, \quad \rho(1,x) = \begin{cases} 1 & x < 0 \\ 1 & x > 0 \end{cases}.$$

The solution [14] of this Riemann problem for $t \geq 1$ consists of piecewise constants dictated by the Rankine-Hugoniot conditions

$$u(t,x) = \begin{cases} \pm\frac{1}{2} & \mp x > c(1-t) \\ 0 & |x| < c(t-1) \end{cases}, \qquad \rho(t,x) = \begin{cases} 1 & |x| > c(1-t) \\ \rho_m & |x| < c(t-1) \end{cases}, \tag{34}$$

with $\rho_m \approx 1.93$ [14].

We leave as Exercise 0.4 the determination of the wave speed c in (34).

Now extend (26) to a system in two space dimensions.

Write $\mathbf{v} = (u, v)$ for the flow variables.

The isentropic, compressible Euler equations can be written as

$$\begin{aligned} \rho_t + \nabla\cdot(\rho\mathbf{v}) &= 0 \\ (\rho\mathbf{v})_t + \nabla\cdot(\rho\mathbf{v}\otimes\mathbf{v}) + \nabla p(\rho)) &= 0, \end{aligned} \tag{35}$$

where $\mathbf{v}\otimes\mathbf{v}$ is matrix with entries $(\mathbf{v}\otimes\mathbf{v})_{ij} = v_i v_j$ and, for matrix-valued function $M(\mathbf{x})$, $\nabla\cdot M$ defined by

$$(\nabla\cdot M)_i = \sum_{j=1}^{d} M_{ij,j}.$$

Bad news

Unfortunately “in more than one space dimension, a good theory for unique continuation of solutions after the formation of shocks is not available” [14].

In particular, [14, Theorem 4, page 125] proves that there are infinitely many “wild solutions” with nonvanishing vorticity

$$\omega(t,x,y) := u_y(t,x,y) - v_x(t,x,y) \neq 0,$$

where $\mathbf{v} = (u, v)$.

The piecewise constant weak solution in (34), extended with $v = 0$, clearly has vorticity equal to zero.

Computational support

Explicit computations are also given in [14] illustrating the behavior of “wild” solutions.

This can be described loosely as the creation of vortices after the collision of two shocks.

Given that the conservation laws are highly idealized models, such an outcome is not surprising.

It should be noted that recent theoretical research on nonuniqueness [1, 7, 10, 12, 13, 14, 15, 16, 17, 35] has focused on weak solutions satisfying entropy conditions.

Entropy conditions not sufficient

Entropy conditions were assumed to select physically relevant solutions for systems of conservation laws.

Now it appears that they do not limit the ambiguity as expected.

It has been known for a long time that general solutions of conservation laws can be described in terms of Young measures [6].

Roughly speaking, at each point in space, the solution set is described in terms of a probability distribution of values.

Young measures

A classical solution in this setting corresponds to the probability measure being a Dirac δ-function, meaning that only one (vector) value is attained.

It is known [28] that, as long as a classical solution of a conservation law exists, the Young measure reduces to a δ-function.

However, after the collision of two shocks, such results are not known, and possible behaviors in such situations could involve non-δ, Young-measure solutions [9].

Such a solution has a definite physical interpretation: Young measure puts limits on solution behavior.

Incomplete theory

Thus it could be very useful to find ways of computing such measure-valued solutions [22].

This area of modeling by PDEs is not fully understood, so we do not attempt to say more about it here.

It seems clear that further research is needed to determine useful simulation models to be used where simple conservation laws were considered sufficient in the past.

But until such improvements are made, multi-dimensional systems of conservation laws must be considered incomplete models.

Exercise 0.1 *Prove that the function $a(t, x)$ defined in (31) satisfies the Rankine-Hugoniot (weak solution) jump condition (11). (Hint: $\gamma(t) = 2(t - 1)$.)*

Exercise 0.2 *Prove that the function b defined in (32) satisfies $b_t = -bb_x$ for $0 \leq t < 1$.*

Exercise 0.3 *Prove that the function b defined in (33) satisfies the Rankine-Hugoniot (weak solution) jump condition (11).*

Exercise 0.4 *Determine the wave speed c in (34).*

References

[1] Amit Acharya, Gui-Qiang G Chen, Siran Li, Marshall Slemrod, and Dehua Wang. Fluids, elasticity, geometry, and the existence of wrinkled solutions. *Archive for Rational Mechanics and Analysis*, 226(3):1009–1060, 2017.

[2] Mark Ainsworth. Dispersive and dissipative behaviour of high order discontinuous galerkin finite element methods. *Journal of Computational Physics*, 198(1):106–130, 2004.

[3] Denise Aregba-Driollet and Roberto Natalini. Discrete kinetic schemes for multidimensional systems of conservation laws. *SIAM Journal on Numerical Analysis*, 37(6):1973–2004, 2000.

[4] Pascal Azerad, Jean-Luc Guermond, and Bojan Popov. Well-balanced second-order approximation of the shallow water equation with continuous finite elements. *SIAM Journal on Numerical Analysis*, 55(6):3203–3224, 2017.

[5] Graeme Austin Bird. Molecular gas dynamics. *NASA STI/Recon Technical Report A*, 76, 1976.

[6] Yann Brenier, Camillo De Lellis, and László Székelyhidi. Weak-strong uniqueness for measure-valued solutions. *Communications in mathematical physics*, 305(2):351, 2011.

[7] Jan Březina, Elisabetta Chiodaroli, and Ondřej Kreml. On contact discontinuities in multi-dimensional isentropic Euler equations. *arXiv preprint arXiv:1707.00473*, 2017.

[8] J. Burns, A. Balogh, D. S. Gilliam, and V. I. Shubov. Numerical stationary solutions for a viscous Burgers' equation. *Journal of Mathematical Systems Estimation and Control*, 8:253–256, 1998.

[9] Gui-Qiang Chen and James Glimm. Kolmogorovs theory of turbulence and inviscid limit of the Navier–Stokes equations in $\mathbb{R}^3$. *Communications in Mathematical Physics*, 310(1):267–283, 2012.

[10] Gui-Qiang Chen, Marshall Slemrod, and Dehua Wang. Fluids, geometry, and the onset of Navier–Stokes turbulence in three space dimensions. *Physica D: Nonlinear Phenomena*, 2017.

[11] R. C. Y. Chin and G. W. Hedstrom. A dispersion analysis for difference schemes: tables of generalized Airy functions. *Mathematics of Computation*, 32(144):1163–1170, 1978.